The Mechanism of Catalpol in Alzheimer's Disease by Modulating Mitochondrial Function Through miR-124-Mediated STIM2

Xin Lv
Jinan University First Affiliated Hospital
Jun Qiu
Jinan University First Affiliated Hospital
Tao Hao
Jinan University First Affiliated Hospital
Haoran Zhang
Jinan University First Affiliated Hospital
Haiping Jiang
Jinan University First Affiliated Hospital
Yang Tan (yangtan0730@163.com)
The Seventh Affiliated Hospital Sun Yat-sen University https://orcid.org/0000-0002-6018-6500

Research Article

Keywords: Alzheimer's disease, Catalpol, miR-124, STIM2, Mitochondria, Reactive oxygen species, Aβ1-42, Hippocampal neurons

Posted Date: May 28th, 2021

DOI: https://doi.org/10.21203/rs.3.rs-526939/v1

Abstract

Alzheimer's disease (AD) is a dementia-related disease with cognitive deterioration and memory impairment. Catalpol was reported to relieve impairments in learning and memory. The present study assessed the functional mechanism of catalpol in AD via miR-124/STIM2-mediated mitochondrial function. Primary hippocampal neurons were isolated and cultured. AD cell model was induced by $A\beta_{1-42}$ and treated with catalpol. APP/PS1 mouse model was established and treated with catalpol and miR-124 agomir. $A\beta_{1-42}$ induced mitochondrial damage and reactive oxygen species (ROS) generation in AD cell model. Catalpol alleviated mitochondrial damage and reduced ROS generation in hippocampal neurons. miR-124 was highly expressed in AD cell model and catalpol inhibited miR-124 expression. Catalpol alleviated $A\beta_{1-42}$ induced mitochondrial damage and ROS generation in hippocampal neurons by inhibiting miR-124 expression. miR-124 overexpression after catalpol treatment promoted mitochondrial damage and ROS generation in hippocampal neurons. miR-124 targeted STIM2. Silencing STIM2 after catalpol treatment promoted mitochondrial damage and ROS generation in hippocampal neurons. Catalpol slowed AD progression via the miR-124/STIM2 axis *in vivo*. The results of the present study indicated that catalpol alleviated mitochondrial damage and ROS generation and thus attenuated AD by regulating miR-124-mediated STIM2.

Introduction

Alzheimer's disease (AD) is a brain disease often occurring in the elderly and causes dementia and frailty (Ballard et al., 2011; Mantzavinos & Alexiou, 2017). AD is a common cause of individual morbidity and mortality and a global health concern (Oboudiyat et al., 2013; Lane et al., 2018). Progressive decline in cognitive abilities such as memory, language and behavior is a distinctive characteristic of AD which can develop into loss of abilities of daily performance (Weller & Budson, 2018). Neuropathologically, the features of AD include abnormal extracellular accumulation of amyloid-β peptide in amyloid plaques and tau protein aggregated in intracellular neurofibrillary tangles (Mendiola-Precoma et al., 2016). Major causes of AD include genetic mutation, aging, external factors and complications of other diseases (R, 2019; Tiwari et al., 2019). AD accounts for 50%-70% of dementia cases among people above 60 years old (Sochocka et al., 2017; Lashley et al., 2018). The incidence rate of AD is 1% among people aged 65 years and 8% among people aged 85 years or above (Reitz, 2015). Given the fact that AD has caused heavy economic and social burdens on patients, novel therapeutic strategies for AD are in urgent need.

Catalpol is an iridoid glucoside widely distributed in many plants (Bai et al., 2019; Bhattamisra et al., 2019). Catalpol could exert anti-oxidation, anti-inflammation, anti-apoptosis and other neuroprotective effects in multiple diseases (Jiang et al., 2015). Previous studies have indicated that catalpol preserves neural function and regulates function of hypothalamic-pituitary-adrenocortical-axis in mice with AD (Wang et al., 2014; Huang et al., 2016). Also, catalpol attenuates mitochondrial dysfunction which is closely associated with AD (Bi et al., 2008; Wang et al., 2014; Huang et al., 2016; Kerr et al., 2017). The accumulation of reactive oxygen species (ROS) and the collapse of mitochondrial membrane potential ($\Delta\Psi m$) induced by amyloid-beta (Aβ)1–42 are blocked by catalpol in cortical neurons in AD (Liang et al.,

2009). Hence, catalpol has significant values in the search of potential therapeutic strategies of AD due to its neuroprotective effect.

miR-124, a neurosystem-specific microRNA (miRNA), plays a regulatory role in the progression of AD (An et al., 2017). miR-124 also regulates mitochondrial activity in amyotrophic lateral sclerosis (Yardeni et al., 2018). Catalpol could regulate miR-124 expression in neurons after ischemia (Zhu et al., 2019). Stromal interaction molecule 2 (STIM2) is also involved in the development of AD (O'Day, 2020). The downregulation of STIM2 protein causes disrupted store-operated Ca^{2+} entry pathway in AD spines, consequently leading to memory loss (Popugaeva et al., 2017). Therefore, this study investigated the potential mechanism of catalpol in attenuating AD via modulating the miR-124/STIM2-mediated mitochondrial function.

Material And Methods

Ethics statement

This study was approved by the Ethics Committee of The Seventh Affiliated Hospital, Sun Yat-sen University. All experiment procedures were approved by the Laboratory Animal Committee in accordance with the guidelines of International Association for the Study of Pain.

Primary culture of primary hippocampal neurons in mice

As previously mentioned (Taylor et al., 2014), mixed cortex and hippocampal neurons were isolated from fetal mice of embryonic day 14–16. The isolated hippocampal neurons were cultured with Dulbecco's modified Eagle's medium (DMEM; Gibco, Grand Island, NY, USA) containing 10% FBS and 1% penicillin-streptomycin (Gibco) in an incubator with 5% CO_2 at 37°C.

Cell treatment and grouping

According to the reference (Zhang et al., 2017), AD cell model was induced using $A\beta_{1-42}$ (5 μM). STIM2 was silenced using recombinant lentivirus eukaryotic expressing plasmid (sh-NC, sh-STIM2) and packaged into lentivirus. Above lentivirus was prepared in large quantities and purified. Corresponding lentivirus was transfected into hippocampal neurons at logarithmic phase when confluence reached 30%. After 48 h of transfection, each well was added with 1 μg/mL puromycin to screen stably-transfected cells. miR-124 mimic or its control (GenePharma, Shanghai, China) was transfected into hippocampal neurons using Lipofectamine 2000 (Invitrogen, Carlsbad, CA, USA) as per the instructions. Catalpol treatment was conducted based on an earlier research (Liu et al., 2018), and the concentration of catalpol used was 500 μM. Cells were assigned into 9 groups: control group, AD group, AD + DMSO group, AD + catalpol group, AD + DMSO + mimic NC group, AD + catalpol + mimic NC group, AD + catalpol + miR-124 mimic group, AD + catalpol + sh-NC group, and AD + catalpol + sh-STIM2 group.

Mitochondrial DNA (mtDNA) content determination

The relative mtDNA content of total DNA extracted from cells was measured using real-time fluorescence quantitative polymerase chain reaction (PCR) analysis by assessing the relative levels of the MT-ND1 gene in mtDNA (F: 5’-CCCTAAAACCCGCCACATCT-3’ and R: 5’-GAGCGATGGTGAGAGCTAAGGT-3’) versus nuclear gene human globulin (F: 5’-GTGCACCTGACTCCTGAGGAGA-3’ and R: 5’-CCTTGATACCAACCTGCCCAG-3’).

Measurement of mitochondrial membrane potential (ΔΨm)

The ΔΨm was measured using JC-1 (5,5',6,6'-Tetrachloro-1,1',3,3'-tetraethyl-imidacarbocyanine ; Beyotime, Shanghai, China) under a fluorescence microscope (Carl Zeiss, Jena, Germany). JC-1 dye was mixed with medium and incubated with specimens at 5 μL/mL in an incubator for 20 min without light exposure. After two washes, cells were observed under the fluorescence microscope. The results were presented as the fluorescence intensity ratio of relative polymerization monomer (red/green).

Measurement of Adenosine triphosphate (ATP) synthesis

A total of 1×10^4 cells were harvested and incubated with 200 μL cell lysis buffer according to the ATP determination kit (Beyotime). Cells were aspirated and centrifuged at 1200 × g for 5 min. Next, 100 μL supernatants were moved to prepared wells for 5 min. ATP luminescence was detected using a microplate reader (Synergy 2 Multi-Mode microplate reader, BioTek, Winooski, VT).

Measurement of ROS production

The process of DCFH-DA and DHR 123 immunofluorescence was as follows. Hippocampal neurons were collected from each group and seeded into 96-microwell plates (237105, Thermo Fisher Scientific, Rockford, IL, USA) at the density of 3×10^4 per well. Total cellular ROS was measured using DCFH-DA (Cell Biolabs, San Diego, CA, USA). After 10 min of incubation with DCFH-DA (10 mM) at 37°C, DCF fluorescence was detected using a fluorescence microplate reader (Infinite F 200, Tecan Japan, Kanagawa, Japan). Based on manufacturer’s instructions, the excitation and emission wavelength was 485 nm and 535 nm, respectively. Mitochondrial ROS generation was determined using dihydrorhodamine 123 (DHR 123) assay. Fluorescence microscope was used for photographing and observation.

Mitochondrial superoxide in the hippocampus was determined (Jia et al., 2016). The hippocampus slices (300 μM) of each group were incubated for 30 min using MitoSOX (5 μM, Invitrogen) to determine mitochondrial ROS level *in vivo*. The fluorescence of oxidative dye in the slices was detected with a laser confocal microscope (TCS-SP2, Leica, Wetzlar, Germany). The excitation and emission wavelength was 498 nm and 522 nm, respectively. The ROS fluorescence values were analyzed using the Leica SP2 software.

Reverse transcription-quantitative PCR (RT-qPCR)

Total RNA was extracted using TRIzol reagent (Invitrogen) according to the instructions. Reverse transcription of RNA and antisense miRNA to cDNA was performed using PrimeScript RT kit (RR037A,

Takara, Tokyo, Japan) with 10 μL reaction system based on the instructions. Reaction solution was used for fluorescence qPCR according to the introductions of SYBR®Premix ExTaqTM kit (RR820A, TaKaRa) using real-time fluorescent quantitative PCR system (ABI 7500, ABI, Foster City, CA, USA). With U6 as an internal control, relative expression of each target gene was calculated using the $2^{-\Delta\Delta Ct}$ method. Each experiment was repeated 3 times. ΔΔCt = ΔCt test group – ΔCt control group and ΔCt = Ct target gene – Ct internal control. Related primers were designed by Sangon Biotech (Shanghai, China) (Table 1).

Table 1
Primer sequences

Name of primer	Sequences
miR-124	F: 5'-UAAGGCACGCGGUGAAUGCC – 3'
U6	F: 5'-CTCGCTTCGGCAGCACATATACT – 3'
	R: 5'-ACGCTTCACGAATTTGCGTGTC – 3'
Notes: miR, microRNA; F, forward; R, reverse	

Western blot

Tissues or cells were collected with trypsin digestion and then lysed with enhanced radioimmunoprecipitation assay (RIPA) buffer (Boster, Wuhan, China) containing protease inhibitor. Protein concentration was detected using the bicinchoninic acid (BCA) kit (Boster). Protein samples were separated using 10% sodium dodecyl sulfate-polyacrylamide gel electrophoresis and transferred onto the polyvinylidene fluoride (PVDF) membranes. After 2 h of blocking with 5% bovine serum albumin (BSA) to block the non-specific binding, diluted primary antibodies STIM2 (ab181258; 1:1000, Abcam, Cambridge, UK) and GAPDH (ab9485; 1:2500, Abcam) were added and incubated with the membranes at 4°C overnight. Then, the membranes were washed and added with HRP labeled goat anti-rabbit (ab6721; 1:2000, Abcam) and incubated for 1 h, followed by incubation of transfer film with ECL working solution at room temperature for 1 min. Excess ECL reagent was removed and the membranes were sealed with fresh-keeping film. X-ray film was placed in the cassette for 5–10 min-exposure before imaging and fixation. The bands of each group in Western blot images were analyzed by Image J software. GAPDH was internal control. Each experiment was repeated 3 times.

Dual-luciferase reporter assay

The 3'UTR dual-luciferase reporter gene vector of STIM2 wild type and mutant-type plasmid containing miR-124 binding sites were constructed. The STIM2-WT, STIM2-MUT, reporter plasmid miR-124 mimic plasmid and negative control plasmid were cotransfected into 293T cells, respectively. Cells were lysed 24 h after transfection and centrifuged at 12000 rpm for 1 min. Supernatants were collected. Luciferase activities were measured using Dual-Luciferase® Reporter Assay System (E1910, Promega, Madison, WI, USA). Each cell sample was added with 100 μL Firefly luciferase working solution to detect Firefly luciferase, and added with 100 μL Renilla luciferase working solution to detect Renilla luciferase. The

Firefly luciferase and Renilla luciferase were taken as relative luciferase activity. Each experiment was repeated 3 times.

Animals and grouping

A total of 30 healthy male APP/PS1 transgenic AD mice aged 3 months (average weight, 28 ± 2 g) and 6 C57BL/6J WT mice (average weight, 26 ± 4 g) of the same background and growth phase were purchased from JKboit (Nanjing, China).

Mice were assigned into 6 groups (N = 6 per group): normal group (C57BL/6J WT mice), APP/PS1 group, APP/PS1 + DMSO group (mice were treated with DMSO gavage), APP/PS1 + catalpol group (mice were treated with catalpol gavage), APP/PS1 + catalpol + agomir NC group (mice were treated with catalpol gavage and stereotactic brain injection of antagomir NC), and APP/PS1 + Catalpol + miR-124 agomir group (mice were treated with catalpol gavage and stereotactic brain injection of miR-124 antagomir). Catalpol (20 mk/kg; Sigma-Aldrich, St. Louis, MO, USA) gavage was performed once per day for 30 days (Huang et al., 2016). miR-124 agomir and agomir NC were purchased from GenePharma. On the first day of catalpol treatment, mice in the APP/PS1 + catalpol + agomir NC group and APP/PS1 + catalpol + miR-124 agomir group were subjected to stereotactic brain injection of miR-124 agomir and agomir NC. Behavioral tests were conducted 30 days after catalpol or DMSO treatment. Mice were killed after behavioral test and peripheral blood was collected. The brain tissues were dissected and collected for histopathological study.

Morris water maze (MWM) test

As previously mentioned (Pei et al., 2015), MWM test was performed to examine the abilities of spatial learning and memory of mice in this study. Briefly, the water maze consisted of a round bathtub (120 cm in diameter and 60 cm in height) and a circular platform (6 cm in diameter) which was submerged 1 cm below the water surface. The bathtub was located in an environment with rich visual hints outside the maze. Mice were given 20 min to adapt to the test environment before experiment. Invisible platform training was performed for 6 days consecutively and each included 4 trials. During each trial, mice were released from the walls of the box and given 60 s to search and stand on the invisible platform. If mice failed to reach the platform in the given time, they would be guided to the platform manually. Orientation navigation experiment was conducted 24 h after training. In this experiment, the platform was removed and performance of each mouse within 60 s was recorded. The escape latency before reaching the platform, the time spent in each quadrant and the times of platform crossing were recorded.

Hematoxylin and eosin (HE) staining

The tissues were embedded in paraffin, fixed on the microtome and sectioned at 4 μm. The slices were placed in water at 46°C and spread, and then dried in a slide drier for 2 h at 72°C. Next, the slices were cooled for 10 min, cleared with xylene I for 10 min and xylene II for 10 min, dehydrated with ethanol I for 5 min and ethanol II for 5 min, followed by 90% ethanol for 2 min, 80% ethanol for 2 min, 70% ethanol for 2 min. After washed with flowing water for 5 min, the slices were stained with hematoxylin for 5–10 min,

washed for 5 min and treated with hydrochloric ethanol for 2–3 s. After washed with flowing water for 5 min, the slices were rinsed with lithium carbonate for 5 min to turn back to blue, washed for 10 min and stained with eosin for 2 min. After washed for 5 min, the slices were treated with 8-% ethanol for 2 min, 90% ethanol for 2 min, absolute ethanol for 2 min, and xylene for 2 min. Finally, the slices were swabbed, sealed with neutral resin and observed under a light microscope.

Statistical analysis

All data were analyzed using SPSS 21.0 statistical software (IBM Corp., Armonk, NY, USA). The normality and homogeneity of variance tests were conducted first. Measurement data were expressed as means ± standard deviation (SD). The data conformed to normal distribution between two groups were compared by independent sample *t* test, while comparison among multiple groups was made by one-way analysis of variance (ANOVA), followed by Tukey's multiple comparisons test. Comparison among multiple groups at multiple time points was made by repeated measures ANOVA, followed by Bonferroni test. $P < 0.05$ was considered statistically significant.

Results

Catalpol inhibited $A\beta_{1-42}$-induced injury in AD cell model by mediating mitochondrial function

Recent study has showed that catalpol exerts neuroprotective effects in AD (Liu et al., 2018). To investigate whether catalpol participates in AD, AD cell model was induced by $A\beta_{1-42}$ and mitochondrial functions were determined after treating AD cell model with catalpol. RT-qPCR showed that mtDNA level was decreased in AD group and increased in AD + catalpol group (Fig. 1A). ΔΨm measurement result showed that ΔΨm in AD group was in green, suggesting decreased ΔΨm and mitochondrial function; on the other hand, ΔΨm in AD + catalpol group was in red, suggesting increased ΔΨm and enhanced mitochondrial function (Fig. 1B). ATP measurement observed decreased ATP generation in AD group, which suggested injured mitochondria; while ATP generation in AD + catalpol group was increased (Fig. 1C). The measurement of ROS generation found that total ROS and mitochondrial ROS generation in AD group were significantly increased while total ROS and mitochondrial ROS generation in AD + catalpol group were decreased (Fig. 1D-E). These results indicated that $A\beta_{1-42}$ treatment resulted in mitochondrial damage in hippocampal neurons and increased ROS generation, while catalpol treatment alleviated $A\beta_{1-42}$-induced mitochondrial damage and reduced ROS generation. Previous studies have showed that miR-124 may affect the development of AD and catalpol could inhibit miR-124 expression (Zhu et al., 2019; Hou et al., 2020). RT-qPCR result showed that miR-124 expression was increased in AD group but decreased in AD + catalpol group (Fig. 1F). Above results indicated that miR-124 was highly expressed in AD cell model and catalpol inhibited miR-124 expression.

Catalpol attenuated $A\beta_{1-42}$-induced injury in AD cell model via miR-124-mediated mitochondrial function

To explore whether catalpol affects AD by inhibiting miR-124 expression, miR-124 was overexpressed in AD cell model treated with catalpol. RT-qPCR result showed that miR-124 expression was remarkably downregulated in AD + catalpol + mimic NC group but upregulated in AD + catalpol + miR-124 mimic group (Fig. 2A). The measurement mtDNA level was increased in AD + catalpol + mimic NC group but decreased in AD + catalpol + miR-124 mimic group (Fig. 2B). The ΔΨm in AD + catalpol + mimic NC was increased and mitochondrial function was enhanced, while ΔΨm in AD + catalpol + miR-124 mimic group was decreased and mitochondrial function was suppressed (Fig. 2C). The mitochondrial ATP generation was increased in AD + catalpol + mimic NC group but decreased in AD + catalpol + miR-124 mimic group (Fig. 2D). The total ROS and mitochondrial ROS generation were decreased in AD + catalpol + mimic NC group but increased in AD + catalpol + miR-124 mimic group (Fig. 2E-F). These results suggested that catalpol treatment on hippocampal neurons alleviated $A\beta_{1-42}$-induced mitochondrial damage and reduced ROS generation by inhibiting miR-124, and miR-124 overexpression after catalpol treatment intensified mitochondrial damage in hippocampal neurons and ROS generation.

miR-124 targeted STIM2

A recent study has showed that STIM2 affects the progress of AD (Deng et al., 2020). Western blot showed that STIM2 was poorly expressed in AD cell model (Fig. 3A). The binding sites of miR-124 and STIM2 were predicted on bioinformatics website Targetscan (Fig. 3B). Dual-luciferase reporter assay showed that luciferase activity in co-transfection group of miR-124 and STIM2-WT was downregulated while no obvious difference was observed in other co-transfection groups of STIM2-MUT ($P > 0.05$, Fig. 3C). To clarify the effect of miR-124, miR-124 expression was detected by RT-qPCR after overexpressing miR-124 in AD cells. The result suggested that miR-124 expression was obviously increased in cells treated with miR-124 mimic (Fig. 3D). Western blot showed that STIM2 expression was downregulated in cells treated with miR-124 mimic (Fig. 3E). These findings revealed that miR-124 targeted STIM2 in AD cell model.

Catalpol inhibited $A\beta_{1-42}$-induced injury in AD cell model through miR-124/STIM2-mediated mitochondrial function

To investigate whether catalpol affects AD by the miR-124/STIM2, mitochondrial function was determined after silencing STIM2 in catalpol-treated cells. Western blot showed that STIM2 expression was decreased in AD + catalpol + sh-STIM2 group (Fig. 4A). RT-qPCR showed that mtDNA level was decreased in AD + catalpol + sh-STIM2 group (Fig. 4B). The ΔΨm was decreased in AD + catalpol + sh-STIM2 group and mitochondrial function was impaired (Fig. 4C). ATP generation was also reduced in AD + catalpol + sh-STIM2 group (Fig. 4D). Meanwhile, total ROS and mitochondrial ROS generation were elevated in AD + catalpol + sh-STIM2 group (Fig. 4E-F). Altogether, these data demonstrated that silencing

STIM2 after catalpol treatment induced mitochondrial damage and ROS generation in hippocampal neurons.

Catalpol mediated AD development and progression through miR-124/STIM2-mediated mitochondrial function in vivo

To study whether the catalpol/miR-124/STIM2 axis participates in AD, APP/PS1 transgenic AD mouse model was established. RT-qPCR and Western blot results showed that miR-124 was upregulated while STIM2 was downregulated in APP/PS1-treated mice, and miR-124 was downregulated while STIM2 was upregulated in APP/PS1 + catalpol-treated mice; miR-124 was upregulated while STIM2 was downregulated in APP/PS1 + catalpol + miR-124 agomir-treated mice (Fig. 5A-B). MWM test showed that the escape latency of APP/PS1-treated mice was prolonged and the time spent in the quadrant of the platform and the number of crossings the platform were reduced; on the other hand, the escape latency of APP/PS1 + catalpol-treated mice was shortened and the time spent in the quadrant of the platform and the number of crossings the platform was increased; the escape latency of APP/PS1 + catalpol + miR-124 agomir-treated mice was prolonged and the time spent in the quadrant of the platform and the number of crossings the platform was reduced (Fig. 5C-E). HE staining revealed that the hippocampal tissue injury was aggravated in APP/PS1-treated mice; the hippocampal tissue injury of mice treated with APP/PS1 + catalpol was alleviated; while that of mice treated with APP/PS1 + catalpol + miR-124 agomir was exacerbated (Fig. 5F). As for ROS expression, in APP/PS1-treated mice, ROS expression was increased while ROS expression was decreased in mice treated with APP/PS1 + catalpol; ROS expression was elevated in mice treated with APP/PS1 + catalpol + miR-124 agomir (Fig. 5G). Collectively, catalpol slowed AD progression through miR-124/STIM2-mediated mitochondrial function.

Discussion

AD is a common cause of dementia and a major cause of death, the diagnosis and treatment of which require careful and comprehensive medical evaluation (Alzheimer's, 2016). Catalpol has been found to play a neuroprotective role in neurodegenerative disorders such as AD and Parkinson’s disease (Jiang et al., 2015). In this study, we investigated the mechanism of catalpol in AD in mice. The result showed that catalpol could mitigate AD progression in mice by regulating the miR-124/STIM2-mediated mitochondrial function.

Catalpol mitigated $A\beta_{1-42}$-induced blood-brain barrier disruption in AD (Liu et al., 2018). In the present study, AD cell model was induced by $A\beta_{1-42}$ to investigate the role of catalpol in mitochondrial function in AD. The alteration of mtDNA has been reported to affect AD pathogenesis (Yan et al., 2013). The mtDNA level in AD cells was decreased while mtDNA level was increased after catalpol treatment. The decreased ATP generation has been reported in AD (Agrawal & Jha, 2020). The result showed that ATP generation was decreased in AD cells while ATP generation was increased after catalpol treatment. Mitochondrial ROS accumulation and loss of $\Delta\Psi m$ were found in AD (Lee et al., 2018). Our study found that total ROS and mitochondrial ROS generation in AD cells were significantly increased while total ROS and

mitochondrial ROS generation were decreased after catalpol treatment. ΔΨm in AD cells was decreased while ΔΨm was increased after catalpol treatment. Catalpol reduces ROS level and enhanced mitochondrial ΔΨm in mice with liver injury, and reduces mitochondrial damage in ischemic injury (Cai et al., 2018; Gao et al., 2020). These results demonstrated that catalpol reduced $A\beta_{1-42}$-induced mitochondrial damage and ROS generation.

miR-124 was recognized as a critical modifier of AD development while catalpol downregulated miR-124 to improve cell viability and neuronal survival (An et al., 2017; Zhu et al., 2019). In this study, miR-124 expression was increased in AD cells but decreased after catalpol treatment. miR-124 plays a negative regulatory role in AD mouse model (Vaz et al., 2020). AD cells were treated with catalpol and miR-124 overexpression to confirm whether catalpol affects AD through miR-124. miR-124 expression was remarkably downregulated in AD cells after treated with catalpol and mimic NC but upregulated after treated with catalpol and miR-124 mimic. The mtDNA level, ΔΨm and ATP generation showed an opposite trend while total ROS and mitochondrial ROS generation showed a uniform trend with miR-124 expression. Mitochondrial dysfunction is also recognized as an early event in AD (Shoshan-Barmatz et al., 2018). miR-124 promotes ROS production in cerebral vascular disease and miR-124 downregulation attenuates mitochondrial dysfunction in myocardial infarction (He et al., 2018; Wang et al., 2018a). Hence, our results indicated that catalpol alleviated mitochondrial damage and ROS generation in hippocampal neurons by inhibiting miR-124 expression.

miR-128 inhibits STIM2 translation and causes memory imprecision in mice with AD (Deng et al., 2020). In this study, the binding sites of miR-124 and STIM2 were predicted on Targetscan website and their target relation was verified by dual-luciferase reporter assay. STIM2 expression was downregulated in AD cells treated with miR-124 mimic. Thus, miR-124 targeted STIM2 in AD cell model. In order to explore whether catalpol affects AD by inhibiting miR-124/STIM2, STIM2 was silenced in catalpol-treated AD cell model. In our study, the mtDNA level, ΔΨm, and ATP generation were decreased while total ROS and mitochondrial ROS generation were elevated after silencing STIM2. ROS generation is minimally impaired in the absence of STIM2 (Clemens et al., 2017). STIM2 overexpression protects against mushroom spine defects in primary hippocampal neurons from AD (Pchitskaya et al., 2017). Increased STIM2 improved neural survival after AD (Sanati et al., 2019). Previous studies have found that lack of STIM2 could result in cognitive impairment and the inhibition of miR-124 could restore memory deficits in AD (Berna-Erro et al., 2009; Wang et al., 2018b). Altogether, catalpol inhibited $A\beta_{1-42}$-induced injury in AD cell model via miR-124/STIM2-mediated mitochondrial function.

APP/PS1 transgenic AD mouse model was established to verify the effect of the catalpol/miR-124/STIM2 axis on AD *in vivo*. In our study, miR-124 was upregulated while STIM2 was downregulated in APP/PS1 mice, which were reversed upon catalpol treatment. The escape latency of APP/PS1 mice was shortened, and the time spent in the quadrant of the platform and the number of crossings the platform were increased after catalpol treatment. The hippocampal tissue injury of APP/PS1 mice was alleviated and ROS expression was decreased after catalpol treatment. Catalpol could relieve learning and memory impairments and improve cognitive function in mice with AD (Huang et al., 2016; Xia et al., 2017). These

results suggested that catalpol slowed AD progression *in vivo*. Essentially, miR-124 agomir treatment in APP/PS1 transgenic AD mice treated with catalpol annulled the protection of catalpol in AD. The suppression of miR-124 in hippocampal neurons enhances cognitive performance (Dutta et al., 2013). Taken together, catalpol slowed AD progression via miR-124/STIM2-mediated mitochondrial function *in vivo*.

In conclusion, our study supported that catalpol alleviated AD by mitigating mitochondrial damage and ROS production through the miR-124/STIM2 axis. Since this study did not provide other potential mechanisms and downstream pathways involving catalpol in AD, further investigations are needed in the field of AD treatment.

Declarations

Ethics approval and consent to participate

This study was approved by the Ethics Committee of The Seventh Affiliated Hospital, Sun Yat-sen University. All experiment procedures were approved by the Laboratory Animal Committee in accordance with the guidelines of International Association for the Study of Pain.

Informed consent

Not applicable.

Competing interests

The authors declare that they have no competing interests.

Consent for publication

Not applicable.

Authors' contributions

XL contributed to the study concepts, study design, and definition of intellectual content; JQ contributed to the literature research; XL contributed to the manuscript preparation and YT contributed to the manuscript editing and review; JQ, TH, HPJ contributed to the experimental studies and data acquisition; HRZ, YT contributed to the data analysis and statistical analysis. All authors read and approved the final manuscript.

Funding

This work supported by Project funded by China Postdoctoral Science Foundation(grant number 2020M673083) and the Opening Research Fund of Guangzhou Key Laboratory of Molecular and Functional Imaging for Clinical Translation(grant number 201905010003).

Availability of data and materials

The data that support the findings of this study are available from the corresponding author upon reasonable request.

References

1. Agrawal I, Jha S (2020) Mitochondrial Dysfunction and Alzheimer's Disease: Role of Microglia. Front Aging Neurosci 12:252
2. Alzheimer's A (2016) 2016 Alzheimer's disease facts and figures. Alzheimers Dement 12:459–509
3. An F, Gong G, Wang Y, Bian M, Yu L, Wei C (2017) MiR-124 acts as a target for Alzheimer's disease by regulating BACE1. Oncotarget 8:114065–114071
4. Bai Y, Zhu R, Tian Y, Li R, Chen B, Zhang H, Xia B, Zhao D, Mo F, Zhang D, Gao S (2019) Catalpol in Diabetes and its Complications: A Review of Pharmacology, Pharmacokinetics, and Safety. *Molecules*, 24
5. Ballard C, Gauthier S, Corbett A, Brayne C, Aarsland D, Jones E (2011) Alzheimer's disease. Lancet 377:1019–1031
6. Berna-Erro A, Braun A, Kraft R, Kleinschnitz C, Schuhmann MK, Stegner D, Wultsch T, Eilers J, Meuth SG, Stoll G, Nieswandt B (2009) STIM2 regulates capacitive Ca2 + entry in neurons and plays a key role in hypoxic neuronal cell death. Sci Signal 2:ra67
7. Bhattamisra SK, Yap KH, Rao V, Choudhury H (2019) Multiple Biological Effects of an Iridoid Glucoside, Catalpol and Its Underlying Molecular Mechanisms. *Biomolecules*, **10**
8. Bi J, Wang XB, Chen L, Hao S, An LJ, Jiang B, Guo L (2008) Catalpol protects mesencephalic neurons against MPTP induced neurotoxicity via attenuation of mitochondrial dysfunction and MAO-B activity. Toxicol In Vitro 22:1883–1889
9. Cai Q, Ma T, Tian Y, Li C, Li H (2018) Catalpol Inhibits Ischemia-Induced Premyelinating Oligodendrocyte Damage through Regulation of Intercellular Calcium Homeostasis via Na(+)/Ca(2+) Exchanger 3. *Int J Mol Sci*, 19
10. Clemens RA, Chong J, Grimes D, Hu Y, Lowell CA (2017) STIM1 and STIM2 cooperatively regulate mouse neutrophil store-operated calcium entry and cytokine production. Blood 130:1565–1577
11. Deng M, Zhang Q, Wu Z, Ma T, He A, Zhang T, Ke X, Yu Q, Han Y, Lu Y (2020) Mossy cell synaptic dysfunction causes memory imprecision via miR-128 inhibition of STIM2 in Alzheimer's disease mouse model. Aging Cell 19:e13144
12. Dutta R, Chomyk AM, Chang A, Ribaudo MV, Deckard SA, Doud MK, Edberg DD, Bai B, Li M, Baranzini SE, Fox RJ, Staugaitis SM, Macklin WB, Trapp BD (2013) Hippocampal demyelination and memory dysfunction are associated with increased levels of the neuronal microRNA miR-124 and reduced AMPA receptors. Ann Neurol 73:637–645

13. Gao X, Xu J, Liu H (2020) Protective effects of catalpol on mitochondria of hepatocytes in cholestatic liver injury. Mol Med Rep 22:2424–2432
14. He F, Liu H, Guo J, Yang D, Yu Y, Yu J, Yan X, Hu J, Du Z (2018) Inhibition of MicroRNA-124 Reduces Cardiomyocyte Apoptosis Following Myocardial Infarction via Targeting STAT3. Cell Physiol Biochem 51:186–200
15. Hou TY, Zhou Y, Zhu LS, Wang X, Pang P, Wang DQ, Liuyang ZY, Man H, Lu Y, Zhu LQ, Liu D (2020) Correcting abnormalities in miR-124/PTPN1 signaling rescues tau pathology in Alzheimer's disease. J Neurochem 154:441–457
16. Huang JZ, Wu J, Xiang S, Sheng S, Jiang Y, Yang Z, Hua F (2016) Catalpol preserves neural function and attenuates the pathology of Alzheimer's disease in mice. Mol Med Rep 13:491–496
17. Jia N, Sun Q, Su Q, Dang S, Chen G (2016) Taurine promotes cognitive function in prenatally stressed juvenile rats via activating the Akt-CREB-PGC1alpha pathway. Redox Biol 10:179–190
18. Jiang B, Shen RF, Bi J, Tian XS, Hinchliffe T, Xia Y (2015) Catalpol: a potential therapeutic for neurodegenerative diseases. Curr Med Chem 22:1278–1291
19. Kerr JS, Adriaanse BA, Greig NH, Mattson MP, Cader MZ, Bohr VA, Fang EF (2017) Mitophagy and Alzheimer's Disease: Cellular and Molecular Mechanisms. Trends Neurosci 40:151–166
20. Lane CA, Hardy J, Schott JM (2018) Alzheimer's disease. Eur J Neurol 25:59–70
21. Lashley T, Schott JM, Weston P, Murray CE, Wellington H, Keshavan A, Foti SC, Foiani M, Toombs J, Rohrer JD, Heslegrave A, Zetterberg H (2018) Molecular biomarkers of Alzheimer's disease: progress and prospects. *Dis Model Mech*, 11
22. Lee J, Kim Y, Liu T, Hwang YJ, Hyeon SJ, Im H, Lee K, Alvarez VE, McKee AC, Um SJ, Hur M, Mook-Jung I, Kowall NW, Ryu H (2018) SIRT3 deregulation is linked to mitochondrial dysfunction in Alzheimer's disease. *Aging Cell*, 17
23. Liang JH, Du J, Xu LD, Jiang T, Hao S, Bi J, Jiang B (2009) Catalpol protects primary cultured cortical neurons induced by Abeta(1–42) through a mitochondrial-dependent caspase pathway. Neurochem Int 55:741–746
24. Liu C, Chen K, Lu Y, Fang Z, Yu G (2018) Catalpol provides a protective effect on fibrillary Abeta1-42 - induced barrier disruption in an in vitro model of the blood-brain barrier. Phytother Res 32:1047–1055
25. Mantzavinos V, Alexiou A (2017) Biomarkers for Alzheimer's Disease Diagnosis. Curr Alzheimer Res 14:1149–1154
26. Mendiola-Precoma J, Berumen LC, Padilla K, Garcia-Alcocer G (2016) Therapies for Prevention and Treatment of Alzheimer's Disease. *Biomed Res Int*, **2016**, 2589276
27. O'Day DH (2020) Calmodulin Binding Proteins and Alzheimer's Disease: Biomarkers, Regulatory Enzymes and Receptors That Are Regulated by Calmodulin. *Int J Mol Sci*, 21
28. Oboudiyat C, Glazer H, Seifan A, Greer C, Isaacson RS (2013) Alzheimer's disease. Semin Neurol 33:313–329

29. Pchitskaya E, Kraskovskaya N, Chernyuk D, Popugaeva E, Zhang H, Vlasova O, Bezprozvanny I (2017) Stim2-Eb3 Association and Morphology of Dendritic Spines in Hippocampal Neurons. Sci Rep 7:17625
30. Pei L, Wang S, Jin H, Bi L, Wei N, Yan H, Yang X, Yao C, Xu M, Shu S, Guo Y, Yan H, Wu J, Li H, Pang P, Tian T, Tian Q, Zhu LQ, Shang Y, Lu Y (2015) A Novel Mechanism of Spine Damages in Stroke via DAPK1 and Tau. Cereb Cortex 25:4559–4571
31. Popugaeva E, Pchitskaya E, Bezprozvanny I (2017) Dysregulation of neuronal calcium homeostasis in Alzheimer's disease - A therapeutic opportunity? Biochem Biophys Res Commun 483:998–1004
32. R AA (2019) Risk factors for Alzheimer's disease. Folia Neuropathol 57:87–105
33. Reitz C (2015) Genetic diagnosis and prognosis of Alzheimer's disease: challenges and opportunities. Expert Rev Mol Diagn 15:339–348
34. Sanati M, Khodagholi F, Aminyavari S, Ghasemi F, Gholami M, Kebriaeezadeh A, Sabzevari O, Hajipour MJ, Imani M, Mahmoudi M, Sharifzadeh M (2019) Impact of Gold Nanoparticles on Amyloid beta-Induced Alzheimer's Disease in a Rat Animal Model: Involvement of STIM Proteins. ACS Chem Neurosci 10:2299–2309
35. Shoshan-Barmatz V, Nahon-Crystal E, Shteinfer-Kuzmine A, Gupta R (2018) VDAC1, mitochondrial dysfunction, and Alzheimer's disease. Pharmacol Res 131:87–101
36. Sochocka M, Zwolinska K, Leszek J (2017) The Infectious Etiology of Alzheimer's Disease. Curr Neuropharmacol 15:996–1009
37. Taylor JM, Minter MR, Newman AG, Zhang M, Adlard PA, Crack PJ (2014) Type-1 interferon signaling mediates neuro-inflammatory events in models of Alzheimer's disease. Neurobiol Aging 35:1012–1023
38. Tiwari S, Atluri V, Kaushik A, Yndart A, Nair M (2019) Alzheimer's disease: pathogenesis, diagnostics, and therapeutics. Int J Nanomedicine 14:5541–5554
39. Vaz AR, Falcao AS, Scarpa E, Semproni C, Brites D (2020) Microglia Susceptibility to Free Bilirubin Is Age-Dependent. Front Pharmacol 11:1012
40. Wang JH, Li WT, Yu ST, Xie H, Han HR (2014) Catalpol regulates function of hypothalamic-pituitary-adrenocortical-axis in an Alzheimer's disease rat model. Pharmazie 69:688–693
41. Wang SW, Deng LX, Chen HY, Su ZQ, Ye SL, Xu WY (2018a) MiR-124 affects the apoptosis of brain vascular endothelial cells and ROS production through regulating PI3K/AKT signaling pathway. Eur Rev Med Pharmacol Sci 22:498–505
42. Wang X, Liu D, Huang HZ, Wang ZH, Hou TY, Yang X, Pang P, Wei N, Zhou YF, Dupras MJ, Calon F, Wang YT, Man HY, Chen JG, Wang JZ, Hebert SS, Lu Y, Zhu LQ (2018b) A Novel MicroRNA-124/PTPN1 Signal Pathway Mediates Synaptic and Memory Deficits in Alzheimer's Disease. Biol Psychiatry 83:395–405
43. Weller J, Budson A (2018) Current understanding of Alzheimer's disease diagnosis and treatment. *F1000Res*, **7**

44. Xia Z, Wang F, Zhou S, Zhang R, Wang F, Huang JH, Wu E, Zhang Y, Hu Y (2017) Catalpol protects synaptic proteins from beta-amyloid induced neuron injury and improves cognitive functions in aged rats. Oncotarget 8:69303–69315
45. Yan MH, Wang X, Zhu X (2013) Mitochondrial defects and oxidative stress in Alzheimer disease and Parkinson disease. Free Radic Biol Med 62:90–101
46. Yardeni T, Fine R, Joshi Y, Gradus-Pery T, Kozer N, Reichenstein I, Yanowski E, Nevo S, Weiss-Tishler H, Eisenberg-Bord M, Shalit T, Plotnikov A, Barr HM, Perlson E, Hornstein E (2018) High content image analysis reveals function of miR-124 upstream of Vimentin in regulating motor neuron mitochondria. Sci Rep 8:59
47. Zhang L, Fang Y, Cheng X, Lian Y, Xu H, Zeng Z, Zhu H (2017) TRPML1 Participates in the Progression of Alzheimer's Disease by Regulating the PPARgamma/AMPK/Mtor Signalling Pathway. Cell Physiol Biochem 43:2446–2456
48. Zhu H, Wang J, Shao Y, Wan D (2019) Catalpol may improve axonal growth via regulating miR-124 regulated PI3K/AKT/mTOR pathway in neurons after ischemia. Ann Transl Med 7:306

Figures

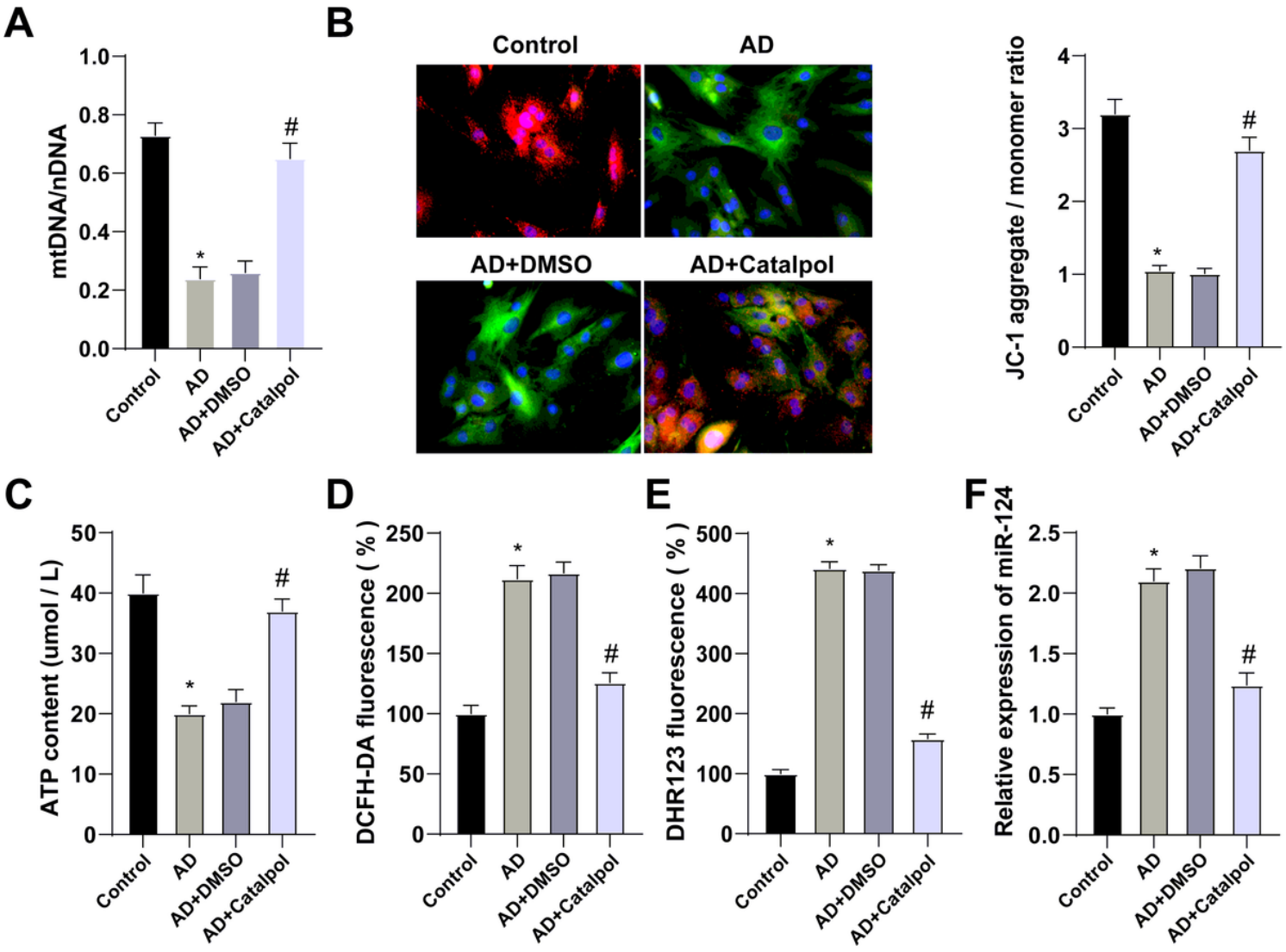

Figure 1

Catalpol inhibited Aβ1-42-induced injury in AD cell model by mediating mitochondrial function. Notes: A: mtDNA level in hippocampal neurons was detected by RT-qPCR; B: ΔΨm change was detected using JC-1 kit; C: ATP generation in hippocampal neurons was detected; D: total ROS generation in hippocampal neurons was detected by DCFH-DA fluorescence; E: mitochondrial ROS generation in hippocampal neurons was detected by DHR123 fluorescence; F: miR-124 expression was detected by RT-qPCR. * $P < 0.05$, compared with AD + DMSO + mimic NC group, # $P < 0.05$, compared with AD + catalpol + miR-124 mimic group. Data in the graphs were measurement data and expressed as mean ± SD. Unpaired t test was performed for pairwise comparison. The experiment was repeated 3 times.

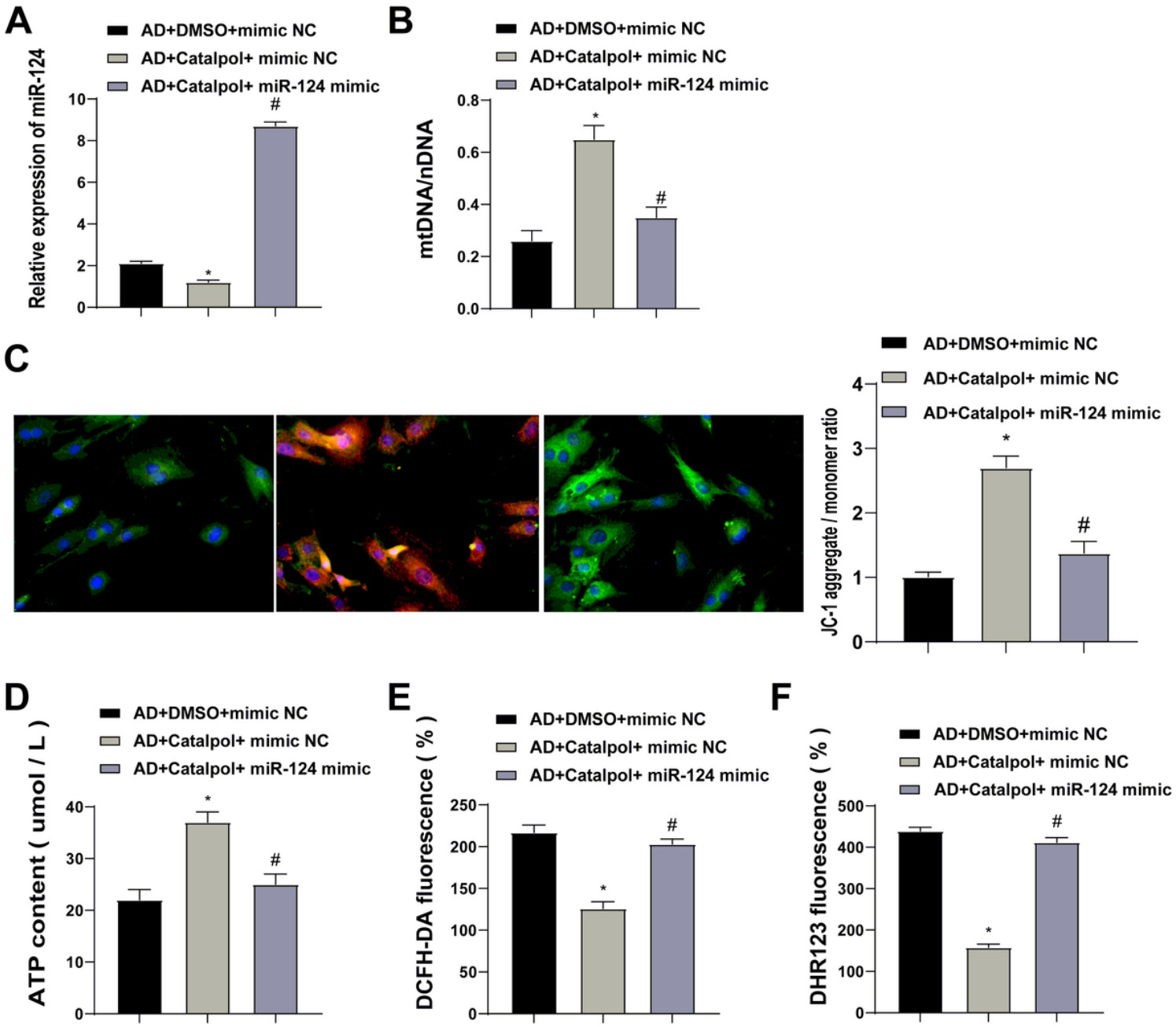

Figure 2

Catalpol attenuated Aβ1-42-induced injury in AD cell model via miR-124-mediated mitochondrial function. Notes: A: miR-124 expression was detected by RT-qPCR; B: mtDNA level in hippocampal neurons was detected by RT-qPCR; C: ΔΨm change was detected using JC-1 kit; D: ATP generation in hippocampal neurons was detected; E: total ROS generation in hippocampal neurons was detected by DCFH-DA fluorescence; F: mitochondrial ROS generation in hippocampal neurons was detected by DHR 123 fluorescence. * P < 0.05, compared with AD + DMSO + mimic NC group, # P < 0.05, compared with AD + catalpol + miR-124 mimic group. Data in the graphs were measurement data and expressed as mean ± SD. Unpaired t test was performed for pairwise comparison. The experiment was repeated 3 times.

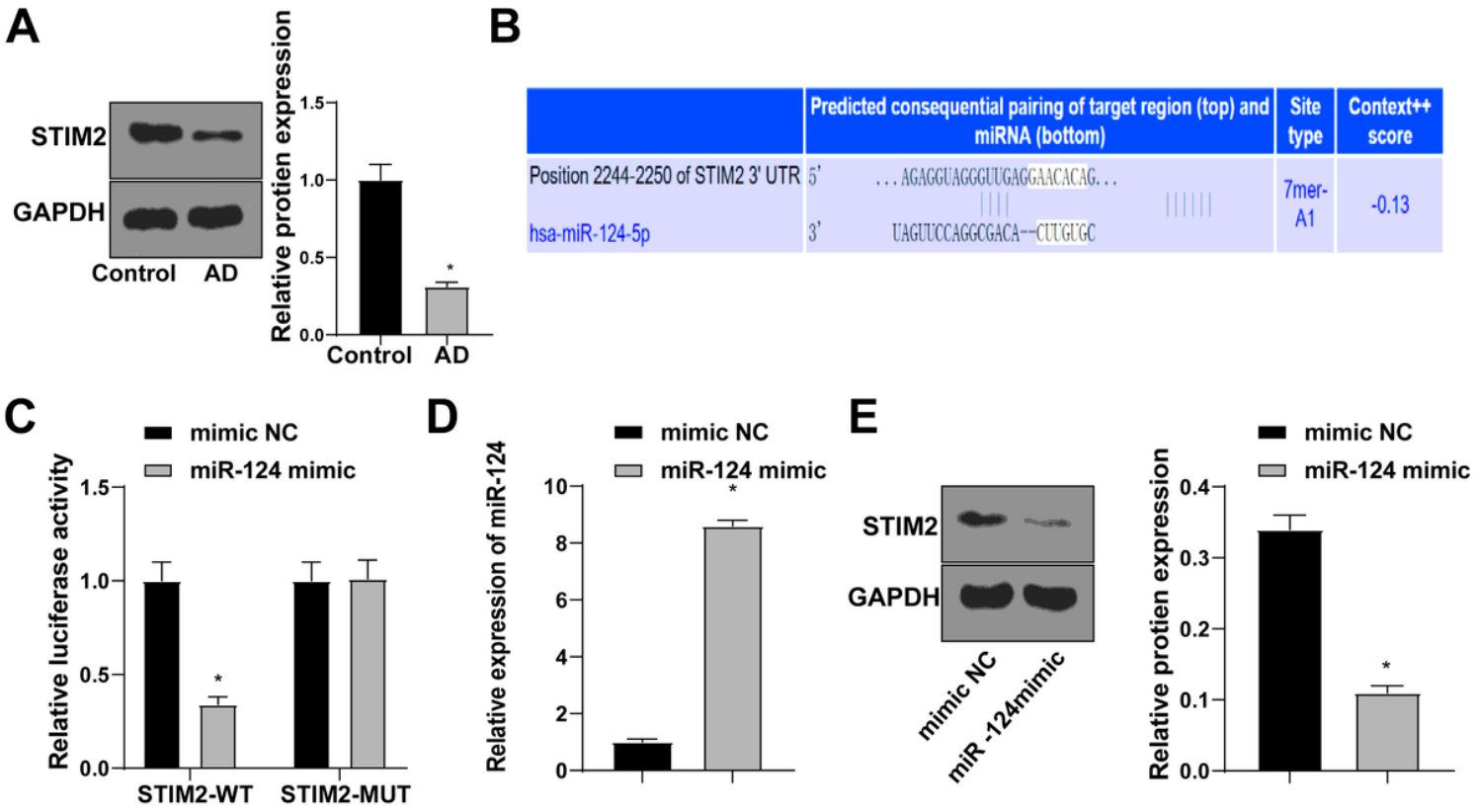

Figure 3

miR-124 targeted STIM2. Notes: A: STIM2 expression in AD cell model was detected by Western blot; B: the binding relation of miR-124 and STIM2 was predicted on bioinformatics website Targetscan; C: the binding relation of miR-124 and STIM2 was verified by dual-luciferase reporter assay; D: miR-124 expression was detected by RT-qPCR; E: STIM2 expression in each group was detected by Western blot. * $P < 0.05$, compared with control group and mimic NC group. Data in the graphs were measurement data and expressed as mean ± SD. Unpaired t test was performed for pairwise comparison. The experiment was repeated 3 times.

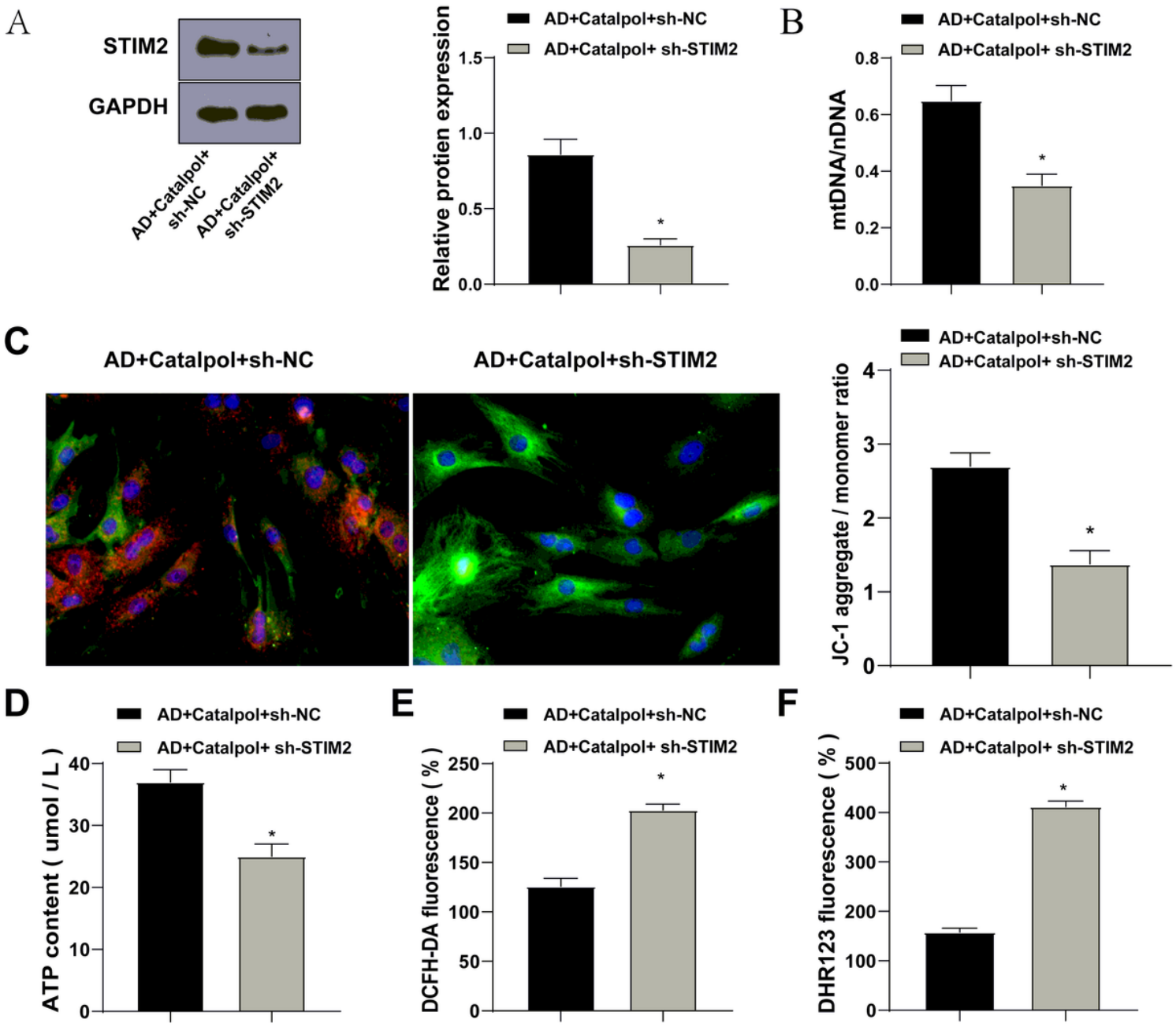

Figure 4

Catalpol inhibited Aβ1-42-induced injury in AD cell model through miR-124/STIM2-mediated mitochondrial function. Notes: A: STIM2 expression in AD cell model was detected by Western blot; B: mtDNA level in hippocampal neurons was detected by RT-qPCR; C: ΔΨm change was detected using JC-1 kit; D: ATP generation in hippocampal neurons was detected; E: total ROS generation in hippocampal neurons was detected by DCFH-DA fluorescence; F: mitochondrial ROS generation in hippocampal neurons was detected by DHR123 fluorescence. * $P < 0.05$, compared with AD + catalpol + sh-NC group. Data in the graphs were measurement data and expressed as mean ± SD. Unpaired t test was performed for pairwise comparison. The experiment was repeated 3 times.

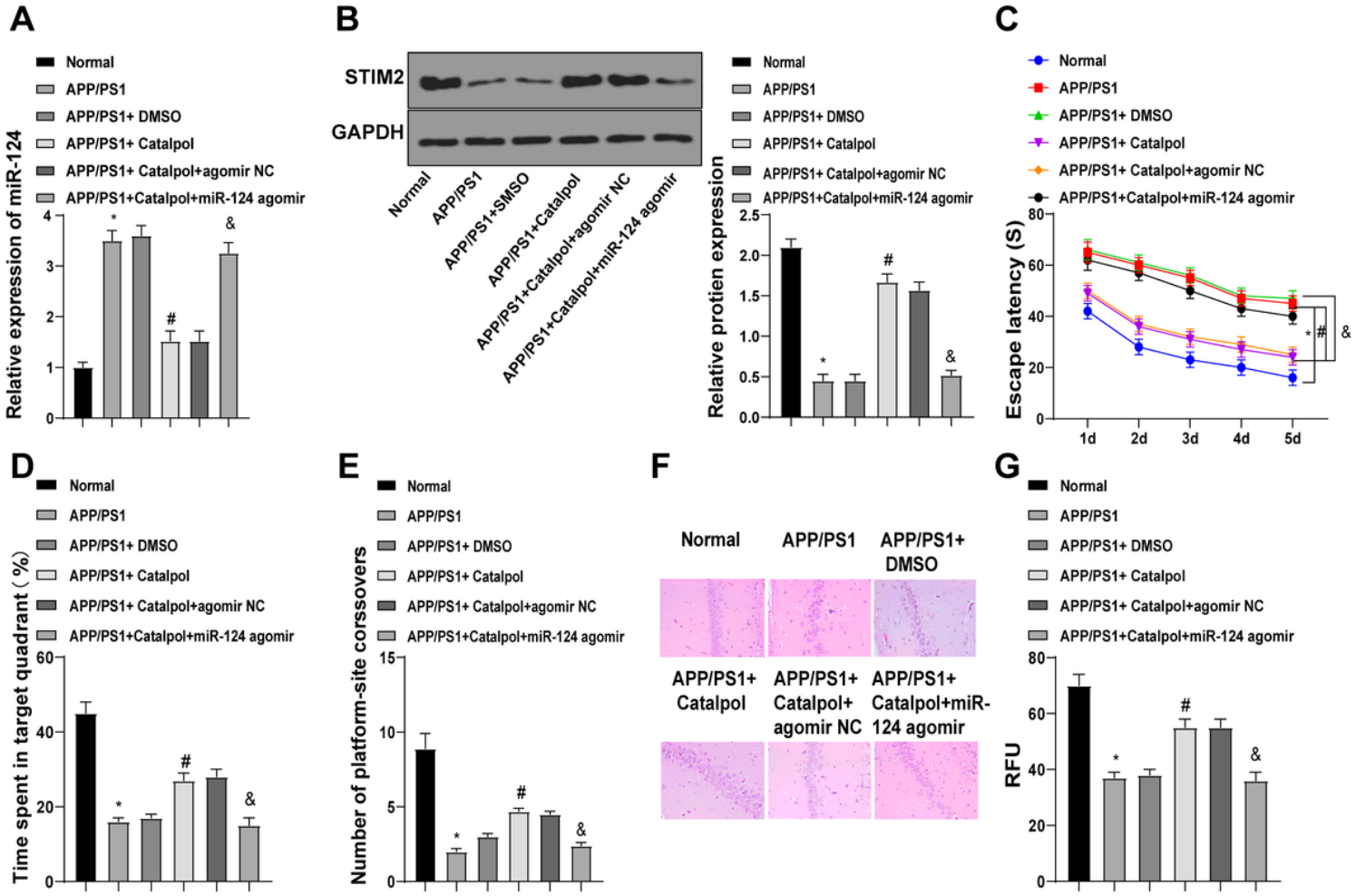

Figure 5

Catalpol mediated AD development and progression through miR-124/STIM2-mediated mitochondrial function in vivo. Notes: A: miR-124 expression in mouse hippocampal tissues was detected by RT-qPCR; B: STIM expression in mouse hippocampal tissues was detected by Western blot; C: escape latency of mice in each group was detected in MWM test; D: the time mice spent in the quadrant of the platform was recorded in MWM test; E: the number of crossings of the platform was recorded in MWM test; F: histopathological conditions of mouse hippocampal tissues were determined by HE staining; G: mitochondrial ROS expression in hippocampal tissues was detected. * $P < 0.05$, compared with normal group, # $P < 0.05$, compared with APP/PS1 + DMSO group, & $P < 0.05$, compared with APP/PS1 + catalpol + agomir NC group. Measurement data were expressed as mean ± SD. Comparison among multiple groups were performed using one-way ANOVA, followed by Tukey's multiple comparisons test. Comparison among multiple groups at multiple time points was made by repeated measures ANOVA, followed by Bonferroni test. N = 6.